Annual Progress Report

The Growth of Gallium Nitride Films via the Innovative Technique of Atomic Layer Epitaxy

Supported Under Contract #N00014-86-K-0686
for the period June 1, 1987 — May 31, 1987

Robert F. Davis,
Michael J. Paisley, and Zlatko Sitar
Materials Science and Engineering
Campus Box 7907
North Carolina State University
Raleigh, NC 27695-7907
(919) 737-3272 or (919) 737-7083

June 1, 1988

UNCLASSIFIED
SECURITY CLASSIFICATION OF THIS PAGE

REPORT DOCUMENTATION PAGE

1a. REPORT SECURITY CLASSIFICATION: Unclassified	1b. RESTRICTIVE MARKINGS: N/A
2a. SECURITY CLASSIFICATION AUTHORITY: N/A	3. DISTRIBUTION/AVAILABILITY OF REPORT: Approved for public release; distribution unlimited
2b. DECLASSIFICATION/DOWNGRADING SCHEDULE: N/A	
4. PERFORMING ORGANIZATION REPORT NUMBER(S): NCSU/MIE-2	5. MONITORING ORGANIZATION REPORT NUMBER(S):
6a. NAME OF PERFORMING ORGANIZATION: North Carolina State Univ. / 6b. OFFICE SYMBOL (If applicable):	7a. NAME OF MONITORING ORGANIZATION: ONR Code 1114
6c. ADDRESS (City, State, and ZIP Code): Dept. of Materials Science and Engr. Box 7907, Raleigh, NC 27695-7907	7b. ADDRESS (City, State, and ZIP Code): Arlington, VA 22217
8a. NAME OF FUNDING/SPONSORING ORGANIZATION: SDIO / 8b. OFFICE SYMBOL (If applicable): IST	9. PROCUREMENT INSTRUMENT IDENTIFICATION NUMBER: N00014-86-K-0686
8c. ADDRESS (City, State, and ZIP Code): Washington, DC	10. SOURCE OF FUNDING NUMBERS: PROGRAM ELEMENT NO: 63220C / PROJECT NO: IST / TASK NO: SRQ / WORK UNIT ACCESSION NO: 001

11. TITLE (Include Security Classification): The Growth of Gallium Nitride Films via the Innovative Technique of Atomic Layer Epitaxy

12. PERSONAL AUTHOR(S): Robert F. Davis

13a. TYPE OF REPORT: Annual	13b. TIME COVERED: FROM 6/1/87 TO 5/31/88	14. DATE OF REPORT (Year, Month, Day): 6/1/88	15. PAGE COUNT: 30

16. SUPPLEMENTARY NOTATION

17. COSATI CODES			18. SUBJECT TERMS (Continue on reverse if necessary and identify by block number)
FIELD	GROUP	SUB-GROUP	

19. ABSTRACT (Continue on reverse if necessary and identify by block number)

This contract involves investigating the efficacy of atomic layer and molecular beam epitaxy techniques for the growth of GaN (a wide direct bandgap semiconductor). During this reporting period, growths on Al_2O_3, α-SiC, and β-SiC were compared. Growths on β-SiC substrates resulted in single crystal thin films of cubic (zinc blende) GaN. Structural analysis by RHEED, TEM, and HRTEM, indicated excellent epitaxy between the SiC substrate and the GaN film.

20. DISTRIBUTION/AVAILABILITY OF ABSTRACT: ☐ UNCLASSIFIED/UNLIMITED ☒ SAME AS RPT ☐ DTIC USERS	21. ABSTRACT SECURITY CLASSIFICATION: Unclassified
22a. NAME OF RESPONSIBLE INDIVIDUAL	22b. TELEPHONE (Include Area Code) / 22c. OFFICE SYMBOL

DD FORM 1473, 84 MAR — 83 APR edition may be used until exhausted. All other editions are obsolete.

SECURITY CLASSIFICATION OF THIS PAGE
UNCLASSIFIED

154-203

Table of Contents

A-1

List of Figures

List of Tables

1. Introduction

1.1 Properties and Applications

Gallium nitride (GaN) is a wide bandgap (3.45 eV at 300K) III-V compound semiconductor. The large direct bandgap and high electron drift velocity of GaN are important properties in the performance of short wavelength optical devices and high power microwave devices. Immediate applications that would be greatly enhanced by the availability of GaN and/or $Al_xGa_{1-x}N$ devices include threat warning systems (based on the ultraviolet (UV) emission from the exhaust plumes of missiles) and radar systems (which require high power microwave generation). Important future applications for devices produced from these materials include blue and ultraviolet semiconductor lasers, blue light emitting diodes (LEDs) and high temperature electronic devices.

Band-to-band transitions in GaN correspond to radiation in the near-ultraviolet region of the spectrum, but by introducing suitable impurities into the material or applying a conventional UV-sensitive phosphor to the finished device (in the case of electroluminescent (EL) applications), it is possible to obtain recombination radiation at various wavelengths throughout the visible spectrum. Extending the laser frequency into the blue regions is very attractive for communications and display applications. Therefore, GaN is potentially useful as a short wavelength semiconductor laser, as an electroluminescent material and as a UV detector. Important applications of this last item include UV solar blind detectors and flame sensors for combustion detection and control.

Gallium nitride also possesses two unique properties required in a semiconductor material to be used in fabricating transit-time-limited (IMPATT, etc.) microwave power amplifiers. It is predicted to have a large saturated electron drift velocity[1] which results in short transit times and thus allows the fabrication of high frequency devices. The basis for this prediction comes from a combination of the relatively small effective electron mass in GaN (m_e= 0.2 m_0), the large optical phonon energy (120 meV) is due to the low mass of nitrogen, and the fact that optical phonon scattering is the primary restriction on the kinetic energy of a hot electron. As a rough approximation, setting $^1/_2\, m_e\, v_s^2 = h\nu_0$, where v_s is the saturated drift velocity and ν_0 is the phonon wave number, one obtains a saturated drift velocity several times greater than either silicon or gallium arsenide.

Also, the bandgap of GaN is more than twice that of GaAs and three times that of Si. Since pair-production thresholds scale with the bandgap, then a GaN transit-time-limited device in reverse bias at high field would be able to operated at higher voltages. This is a result from devices of this

type having to be operated at just below the threshold of pair production. In power amplifiers, the power scales as the square of the voltage, thus GaN would have a significant advantage over Si or GaAs.

1.2 Limitations

Utilization of GaN has been very limited to date because all material produced to date has possessed an intrinsic n-type carrier concentration of at least 10^{17} cm^{-3} and normally more in the range of 10^{18} –10^{19} cm^{-3}. The only high resistivity single crystal material produced has required compensation with a p-type dopant (usually Zn). However, this approach greatly reduces the electron mobility in the film. In addition, intentional growth of p-type GaN has never been achieved, and so devices requiring p-n junctions cannot be produced. (All diode structures produced to date have been metal-insulator-semiconductor (MIS) structures.)

It is a nearly universal consensus that the n-type character is caused by N vacancies produced during the growth process. The basis for this reasoning is that GaN decomposes at ≈1123K at a N_2 pressure of 1 atm. The vapor pressure of N_2 over GaN at 1323K (a common growth temperature used in chemical vapor deposition (CVD) growth of GaN) is 100 atm. Thus molecular nitrogen is not used as a source in CVD growth of GaN. A commonly used nitrogen source in CVD growth is ammonia (NH_3). The equilibrium vapor pressure of NH_3 over GaN at 1323K is only 650 Pa,[2] thus allowing the GaN to form at those elevated temperatures.

2. Nitrogen Source

As mentioned above, the most common source of nitrogen for growth of GaN has been ammonia with hydrazine and certain azides used much less frequently. Since semiconductor grade purities of these materials are nearly impossible to obtain, it was decided to begin work using molecular nitrogen as a source. The nitrogen source finally selected was using the boiloff from a liquid nitrogen dewar which was subsequently passed through a heated copper gas purifying furnace* After passing through a regulating UHV leak valve† which also provided positive shut off, the nitrogen gas traveled into one of the sources described below.

* Model 2B-20-Q, Centorr Associates, Inc., Suncook, NH 03275

† Series 203 Variable Leak, Granville-Phillips Co., Boulder, CO 80303-1398 or Model 951 Variable Leak Valve, Varian Vacuum Products Division, Palo Alto, CA

2.1 RF Plasma Source

Initial attempts at growth of GaN thin films utilized a RF power supply§ operating at 13.56 MHz with a maximum output power of 300 W. The power supply was attached to an inductively wound coil around the glass plasma source, though this apparently still produced capacitive coupling to the plasma.[3] The glass source was mounted in place of a normal effusion cell of the MBE and is shown schematically in the figure below.

This source produced no measurable deposition of GaN on the substrate surface which was covered with large amounts of free gallium on the surface. This gallium coalesced into large droplets upon heating the substrates to remove them from the molybdenum blocks. Subsequent removal of the gallium by chemical etching left no evidence of the formation of a GaN layer on the substrate surface. For this reason, no further analytical work was performed on these substrates and research was begun on a suitable replacement source.

2.2 Microwave Source

In discussions with persons at a plasma diagnostics conference,[4] it was suggested that a microwave source might provide a reaction path better suited to the production of atomic nitrogen. In addition, Kolts and Setzer reported that microwave sources were very effective in producing atomic nitrogen species.[5] In additional discussions with Dr. R. Chrenko at General Electric Research Labs (who is engaged in research which requires atomic nitrogen), it was suggested that a home microwave oven might be suitably modified to provide the microwave energy.

A small 500 W oven was purchased and a small (≈40 mm diameter) hole was cut in the back of the oven for the end of the glass source tube to protrude into the oven cavity. It was fitted with a small section of wire mesh to limit the leakage of microwave energy. A second hole (≈7 mm) was made across from the location of the end of the magnetron tube to allow the entry of an aluminum reflector attached to a rod protruding out of the cavity to allow the oven cavity to be "tuned" for maximum microwave absorption in the plasma. The rod was fitted with a ground wire to minimize microwave leakage.

§ Model HF-300, ENI Power Systems, Inc., Rochester, NY 14623

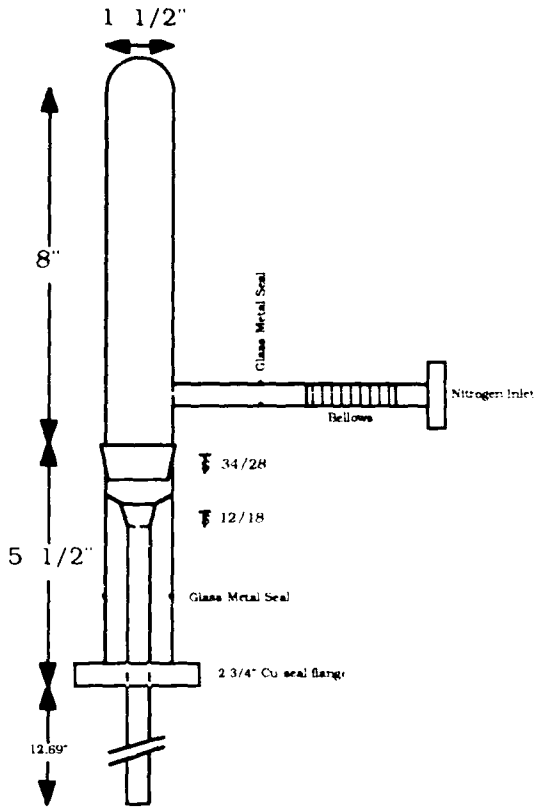

Figure 1. Schematic drawing of glass plasma source used with RF power supply (13.56 MHz and 300 W) to produce activated nitrogen for growth of GaN thin films.

A plasma was achieved with some difficulty but it was not stable or reproducible. Once a good discharge was established, it would not remain stable. After a period of 0.25–0.5 h, the discharge would begin to pulse off and on with a period of 10–30 s. In addition, the microwave oven had a half-wave rectifier on the magnetron tube which likely caused the plasma to ignite and extinguish 60 times per second. Finally, the design of the glass envelope meant that only a fraction of the nitrogen would be directly excited by the microwave energy, thus reducing the amount of atomic nitrogen produced. On this basis a second microwave source was purchased.

The second power supply* (100 W max) and its associated applicator cavity** were attached to a second glass source designed to work with the

* Model MPG-4, Opthos Industries, Inc., Rockville, MD 20855.

** McCarroll-type, Opthos Industries, Inc., Rockville, MD 20855. See articles in reference 3 or more information on this type of cavity.

new cavity design. The microwave cavity was designed specifically for production of plasmas in flowing gases at reduced pressures.[6]

The design of the glass enclosure for the nitrogen plasma changed in several important respects. The changeable orifice was removed in preference to a fixed design that no longer required the wax seal. The wax seal while reasonably effective, was always a deterrent to effective bakeout of the system due to the low melting point of the wax. Although the wax had a very low vapor pressure, it was also viewed as a potential source of hydrocarbon contamination. The plasma chamber was much smaller in diameter, changing from 38 mm in diameter to 13 mm. This change was made to accommodate the size of the new applicator cavity. Finally, because the cavity was a two-piece design, it was possible to design a chamber where 100% of the nitrogen passed directly through the ionizing radiation. The design of the new source is shown in Figure 2.

Initial operation showed that it produced a strong nitrogen plasma after ignition with a Tesla coil (part of normal operation). The first cavity used was defective and produced a strong yellow emission color most likely from sodium in the glass. The presence of sodium in the plasma was of great concern, though after failure of the cavity it was determined that the stimulation of sodium was not normal. A replacement cavity was received with a different kind of metallic plating (nickel) which worked better than the old brass plating. The yellow coloration has disappeared, and concern over sodium incorporation from the glass is reduced.

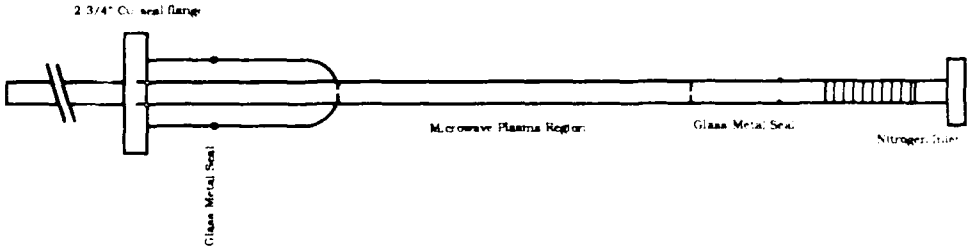

Figure 2. Schematic diagram of the glass nitrogen glow discharge source. The microwave applicator is not shown.

3. Growth Results

3.1 Sapphire (0001) Substrates

Growth studies were undertaken using (0001) Al_2O_3 substrates[§] for comparison to other studies which primarily used sapphire as a substrate material. The substrates (25 mm × 1 mm) were cleaned in 1:1 solution of H_2SO_4:H_2O_2 and then mounted and processed as described in an earlier report.[7] RHEED on the as-grown film indicated the presence of a single crystal material. In addition, it appeared to be of sufficient thickness to no longer show the diffraction pattern of the underlying sapphire. After removal of the sample, it was scribed and fractured into separate pieces for analysis. Scribing the film surface indicated that the film adhered poorly to the substrate. Optical microscopy of the films grown on sapphire indicated the presence of small (≈1 μm diameter) discrete droplets of excess gallium widely separated on the film surface. Examination in the SEM revealed that the surfaces had an uneven morphology as can be seen from the micrograph shown in Figure 3.

Samples were then evaluated in a scanning Auger microscope (JAMP-30, JEOL) for determination of the elemental composition of the grown material. As can be seen in the Auger analysis shown in Figure 4, the material is primarily GaN but readily picked up a surface contamination layer containing oxygen and carbon and does not seem to show any other contaminants to the resolution of the instrument (typically ≈0.1 monolayer).

The samples were then depth profiled in the Auger microscope to determine overall purity and estimate film thickness. Figure 5 shows the results of the depth profile.

A calibration factor for the sputtering rate of GaN has not yet been determined, thus the estimate for the thickness is somewhat crude. However, the best estimate is that the films were ≈30 nm thick. This estimate was roughly verified by transmission optical spectroscopy.

It can be seen that the carbon contamination resided on the surface and was presumably due to atmospheric exposure as the sample received no other treatments. The oxygen signal dropped and was presumably an effect of atmospheric exposure as well. All elemental signals were suppressed as the sapphire substrate was reached due to charging effects (sapphire is an excellent insulator).

[§] Basal plane (0001) orientation, Crystal Systems, Inc., Salem, MA 01970

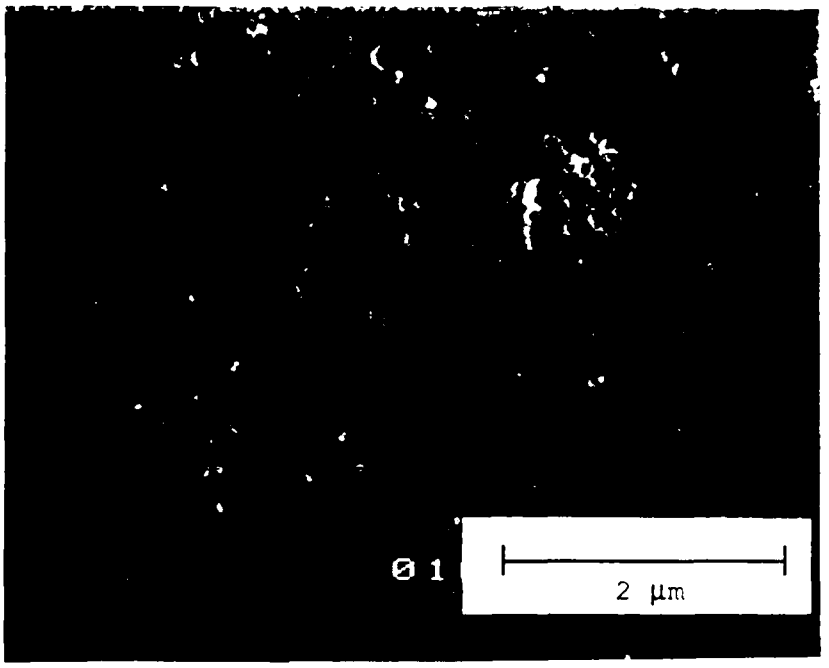

Figure 3. Scanning electron micrograph of surface of GaN film grown on (0001) sapphire substrate (25 kV).

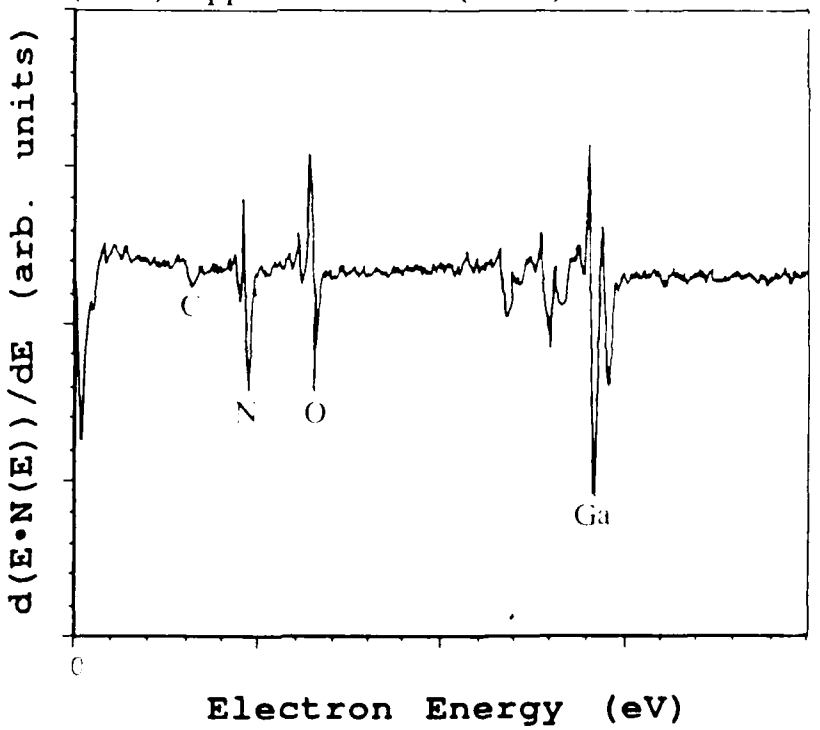

Figure 4. Auger analysis of unsputtered GaN film surface on a sapphire (10 kV).

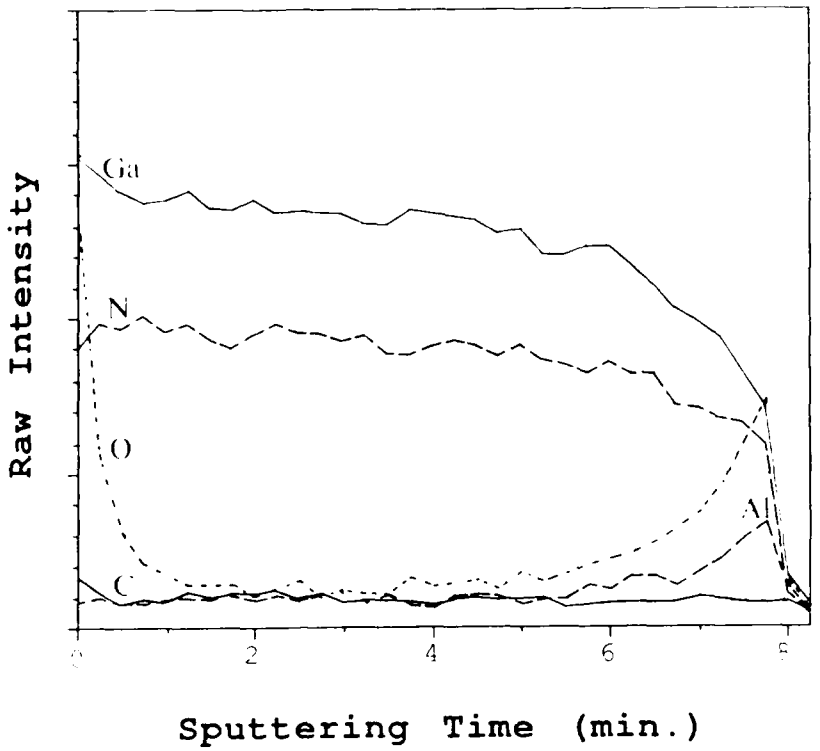

Figure 5. Auger depth profile of GaN on sapphire substrate showing elements C, N, O, Al, and Ga. Note charging effects in the sapphire eliminate all elemental signals as the interface is reached. (10 kV)

The apparent depth of the oxygen signal into the grown film from the substrate was postulated as being due to a sputtering effect. The sputtering process would open holes in the film down to the substrate allowing the oxygen signal to be detected sooner than expected. This is due to roughness in the film surface accentuated by the sputtering action. The aluminum signal indicates a similar behavior though to a lesser extent. In addition, a similar effect is seen for the case of GaN on β-SiC (see below). Due to the extreme fragility of the GaN layer (see above) no further analyses were performed on these films.

3.2 Alpha-Silicon Carbide (0001) Substrates

The (0001) α-SiC substrate used was a horizontal slice (≈1 mm × ≈18 mm in diameter) from a bulk crystal of α-SiC grown in a sublimation furnace designed expressly for this purpose. The crystal was tinted a deep blue due to aluminum present in the crystal. The substrate was subsequently ground and polished ending with a 0.1 μm diamond polish. The substrate was then chemically cleaned and processed as described later for the β-SiC substrates.

The resulting film appeared to be hexagonal from the appearance of the RHEED pattern, though poor substrate mounting prevented much of the pattern from appearing on the screen. Cross-section TEM samples were prepared from this substrate and the results are shown below. Figure 6 shows the good epitaxy between the (6H) α-SiC and the GaN film, though there still appeared to be an oxide layer at the interface which reduced the quality of the deposited GaN. Selected area diffraction of the material indicated single crystal hexagonal GaN that is highly twinned.

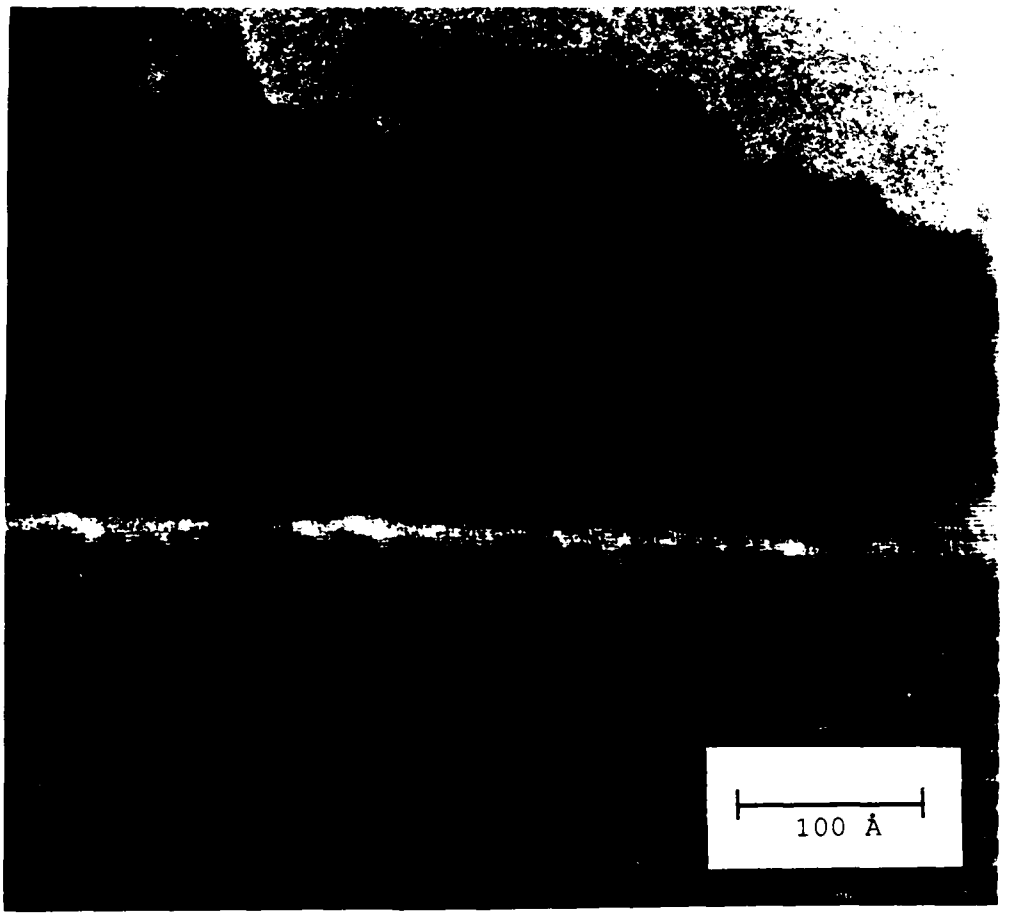

Figure 6. HRTEM photograph of GaN on (0001) α-SiC. Lattice fringes cross interface indicating good epitaxy. This GaN is more defective when compared to GaN on β-SiC.

3.3 Beta-Silicon Carbide (100) Substrates

Growth studies were conducted on (100)-oriented β-SiC substrates. (This material has the cubic zincblende structure.) The β-SiC films were epitaxially grown on (100) Si substrates by CVD of Si and C from pyrolysis of highest purity SiH_4 and C_2H_4 entrained in H_2, in an rf-heated cold-wall barrel-type reactor designed and constructed in house especially for this purpose. The growth temperature was 1360°C and growth rates were typically 2 μm/h. The films were deposited for 2–3 h so that the SiC film upon which the GaN was grown was ≈4–6 μm. The substrates were subsequently polished with 0.1 μm diamond paste and then oxidized at 1200°C in flowing dry oxygen for 1.5 h to consume the 50 nm of surface which contained polish damage.

Below in Table 1 is shown the typical conditions used during growth.

Table 1. Range of conditions used in GaN thin film growth

Nitrogen pressure	5×10^{-6} - 8×10^{-5} Torr
Microwave power	2 - 100 W
Gallium temperature	800 - 950°C
Substrate temperature	500 - 700°C
Growth time	120 – 480 min.

RHEED of the film just after growth as shown in Figure 7 indicated the presence of a single crystal material. The pattern also seems to indicate the presence of twins in the GaN because of the extra spots at the $^1/_3$ position as noted by the white index numbers. In addition, it appeared to be of sufficient thickness to no longer show the diffraction pattern of the underlying β-SiC.

Figure 8 shows a time sequence of [110] RHEED photographs taken at selected times during the growth of a GaN film on a β-SiC substrate. The streaks in the photograph before growth are due to the flatness of the substrate (and its quality). These streaks disappeared due to the formation of growth islands of GaN which developed as deposition began. The growth islands disrupted the electron beam sufficiently that the streaks were no longer visible. These islands were seen in SEM photographs shown in an earlier report.[8] The next features that became apparent in this time sequence were the satellite spots due to ⟨111⟩-type twins/stacking faults that formed in the GaN layer. These twins/faults appeared to diminish in intensity as the growth of the GaN progressed. This decrease in intensity would likely mean that the twins were become less dense in the growing film. Finally, the streaks reappear as the growth interface smooths out again.

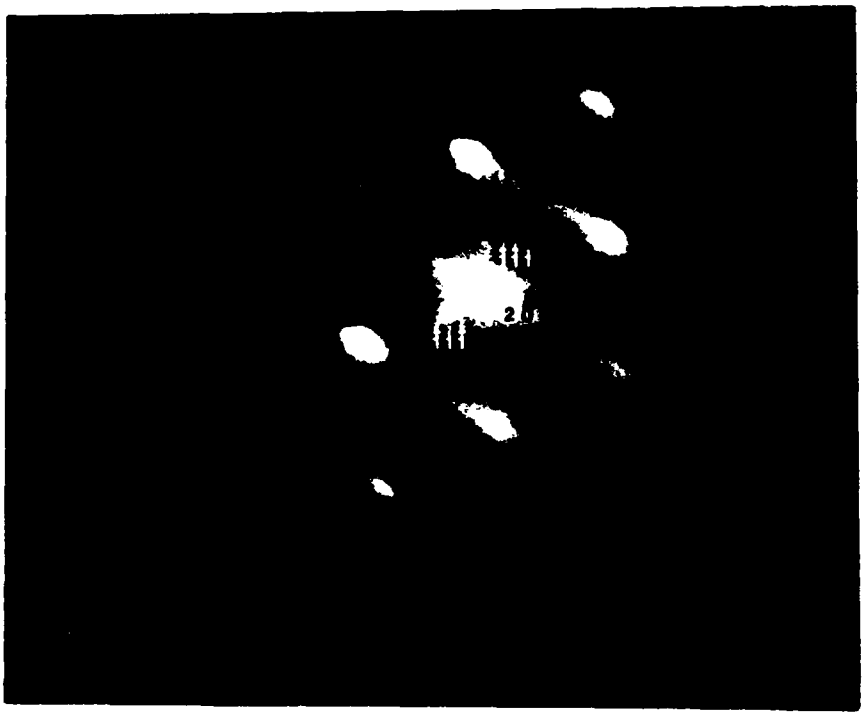

Figure 7. RHEED pattern of GaN film on β-SiC (100) during growth. Electron beam was parallel to [011] direction. White numerals denote twin spots.

The [110] pattern of the β-SiC did not appear to shift orientation as the GaN was depositing, thus indicating that the GaN layer was in fact the cubic zincblende structure as was the β-SiC. The lattice parameter mismatch of the two materials is only ≈3–4%, thus no linear shift in the spot pattern was observed in the RHEED pattern. Only thin layers of polycrystalline cubic GaN have previously been reported in the literature.[9] with an additional reference to unpublished research with a lattice parameter of 4.51 Å for cubic GaN.[10]

After removal of the sample, it was cleaved into separate pieces for analysis. A diamond scribe was used to evaluate the film adherence and indicated that adherence was much better than that for GaN on sapphire (see above). Optical microscopy of the films grown on β-SiC showed a much smoother top surface and no indication of the presence of gallium droplets on the film surface. Examination in the SEM revealed that the surfaces had an uneven morphology (but smoother than films grown on sapphire) as can be seen from the micrograph shown in Figure 9.

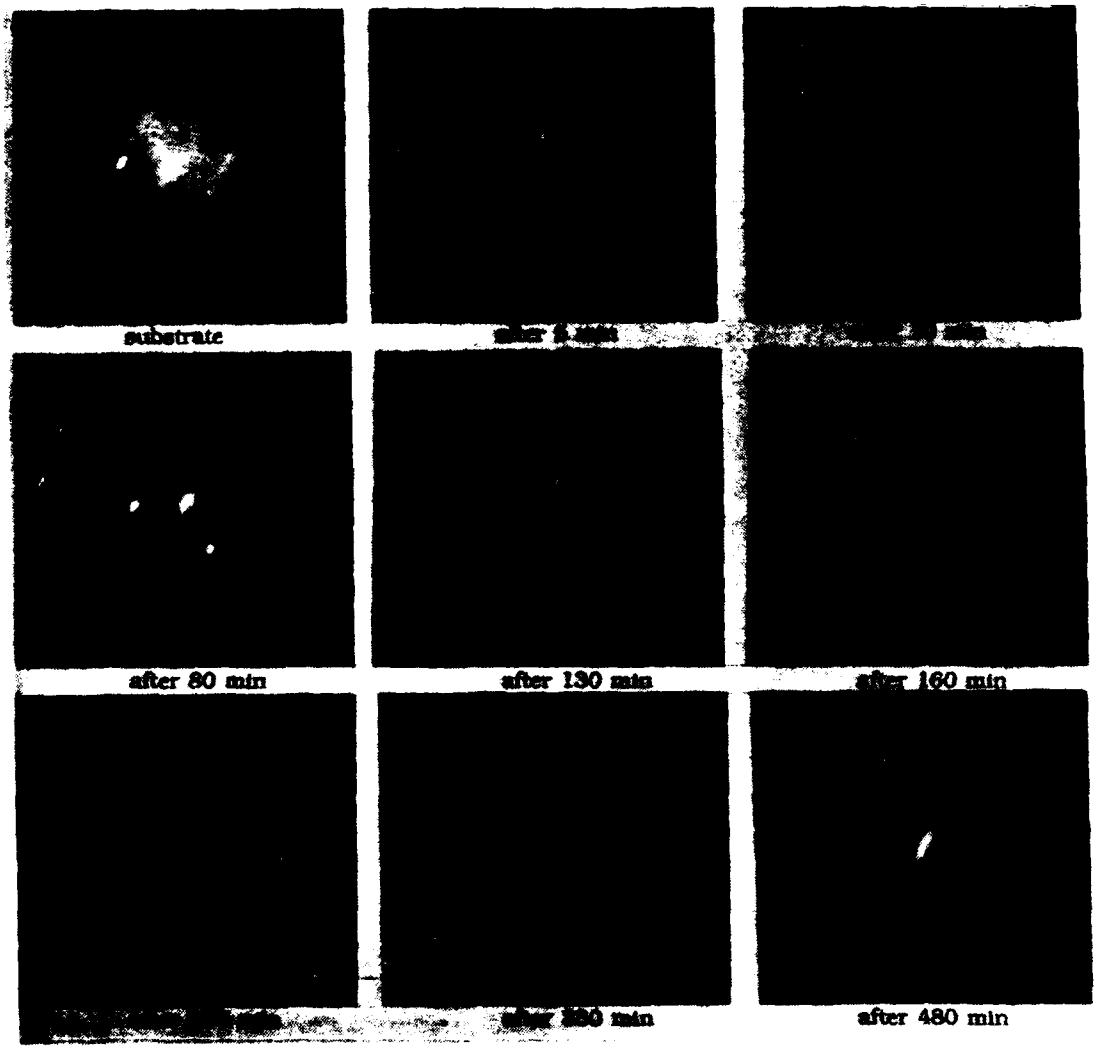

Figure 8. Time sequence of [110] RHEED photographs before, during, and after the growth of a GaN layer on a (100) β-SiC substrate. Initial streaks due to flat substrate surface disappear as growth islands develop. Streaks reappear as growth surface becomes more smooth.

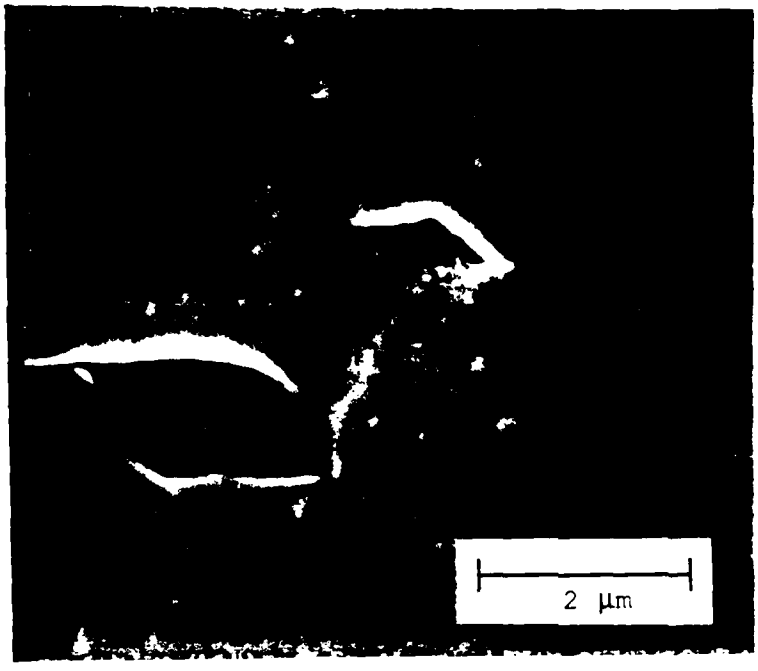

Figure 9. Scanning electron micrograph of surface of GaN film deposited on β-SiC substrate (25 kV).

Evaluation of the samples continued in the scanning Auger microscope to determine the elemental composition of the deposited layer. The Auger analysis in Figure 10 shows the material is primarily GaN. However, a surface contamination layer containing oxygen and carbon was observed. No other contaminants within the resolution of the instrument—typically ≈0.1 monolayer were detected. The carbon level appears higher and the oxygen level lower than in the case of growth on basal (0001) sapphire (see discussion).

The samples were subsequently depth profiled in the Auger microscope to determine overall purity and to estimate the film thickness. Figure 11 shows the results of the depth profile.

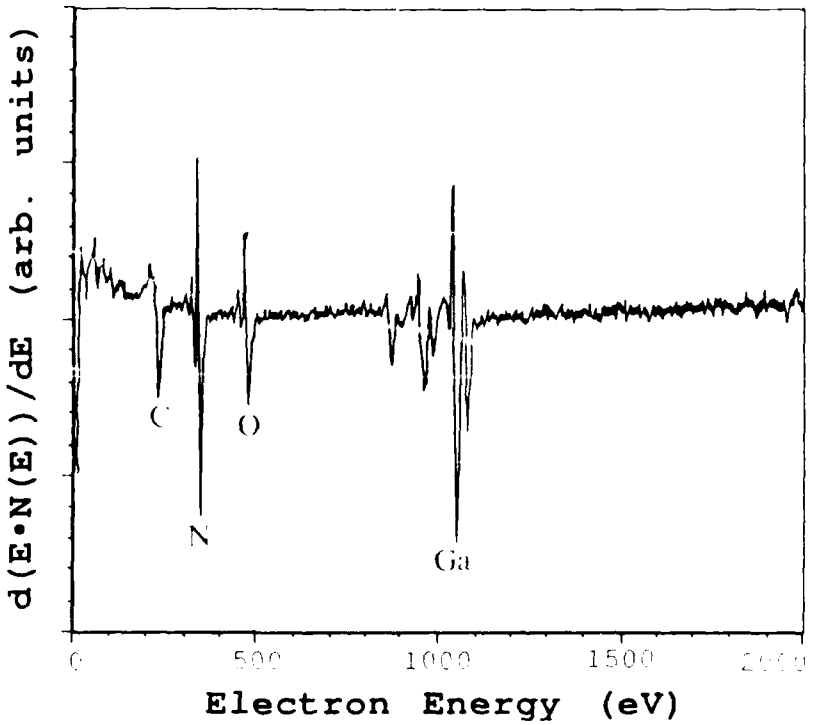

Figure 10. Auger analysis of unsputtered GaN on β-SiC (100) substrate. Note oxygen and carbon contamination which resides only on film surface. (5 kV)

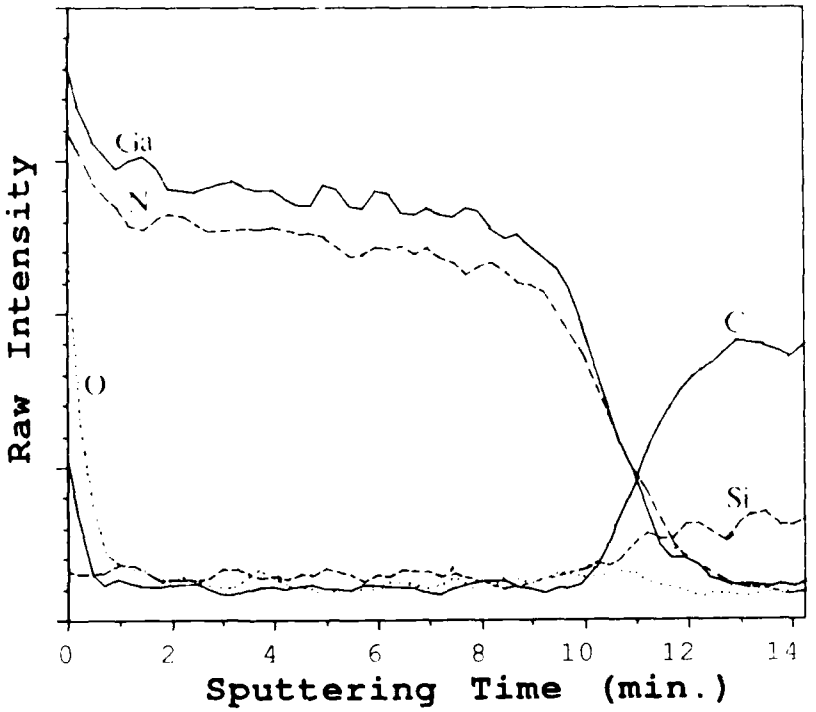

Figure 11. Auger depth profile of GaN film on (100) β-SiC substrate showing elements C, N, O, Si, and Ga. (5 kV)

The depth profile shows that the carbon and oxygen contamination resided on the surface and was presumably due to atmospheric exposure, as discussed for the deposition on sapphire. No suppression of signal was seen as the depth profiling passed through the GaN-SiC interface, since the β-SiC is much more conductive than the sapphire. The apparent depth of the Si and C signals into the GaN film was postulated as being due to the same sputtering process described earlier for the depth of the oxygen signal into the GaN on sapphire.

The next analysis undertaken was transmission electron microscopy in plan and cross sectional orientations. Plan view samples were not very informative due to the fact that the foil preparation procedures produced only samples which had no areas with only GaN. Thus Moiré fringes and related effects made it nearly impossible to determine what was structure in the GaN and what was structure in the β-SiC. However, it was determined that the areas did appear uniform and thus details described below in the cross section samples were not artifacts of an unusual location on the samples.

Figure 12 is an indexed selected area diffraction pattern of the GaN/β-SiC layer. Higher order spots separate into two spots, one sharp spot from the β-SiC and one more diffuse spot from the GaN. Analysis of the SAD patterns (along with convergent beam diffraction of each layer separately) showed that the GaN layer was in fact cubic with a lattice parameter of ≈4.54 Å ±0.04. This agrees within experimental error with a value reported by Pankove[10] for unpublished work on polycrystalline cubic GaN material. This value is slightly larger than that of 4.3596 Å for β-SiC.

Figure 13 below shows a cross-section TEM photograph of the GaN layer. The presence of microtwins is shown by the ⟨111⟩-direction streaking in the diffraction pattern. Note the highly defective region closest to the β-SiC surface. The presence of {111}-type twins is borne out by the following figures showing complementary dark-field images where the twins are clearly delineated. Note that the density of defects appears quite high at the interface and drops off rapidly after a few hundred angstroms of growth. This implies that low defect density GaN layers are possible, and the many of the defects are related to problems at the interface.

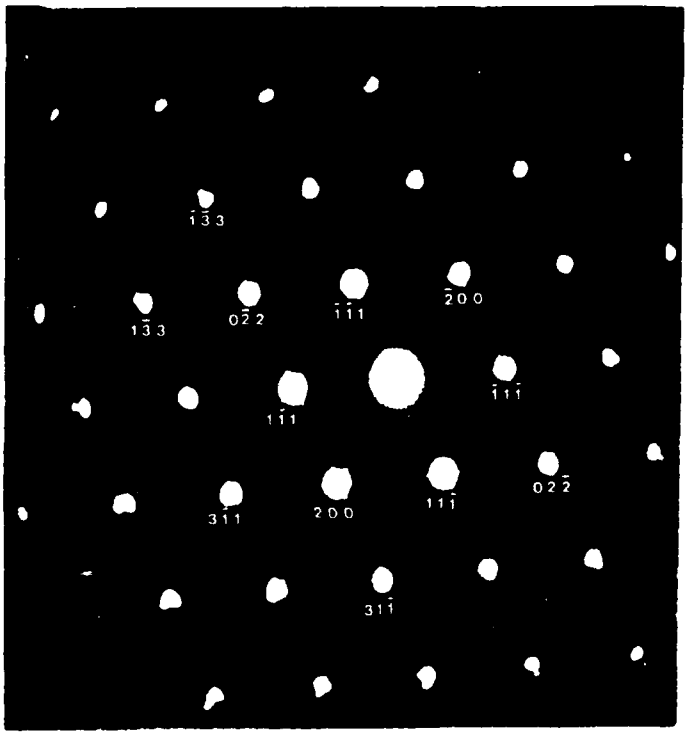

Figure 12. Selected area diffraction pattern in the [011] direction of both β-SiC and GaN. Double spots are observed at the higher order spots. The sharp diffraction spots are from the β-SiC and the more diffuse spots are from the GaN.

Figure 15 shows a high resolution TEM photograph of the β-SiC/GaN interface. The good epitaxy between the β-SiC and the GaN is quite apparent as the lattice fringes line up quite well across the interface. Also visible are the microtwins/stacking faults seen earlier in both the RHEED and XTEM photographs. Again, it appears that many of these defects terminate within a few hundred angstroms of the interface. There is a dark band of approximately three fringe thicknesses that runs directly along the interface between the β-SiC and GaN. This would likely be the source of many of the defects observed in the GaN and most likely be due to remaining native oxide on the β-SiC substrate. The following LEED pattern in Figure 16 shows evidence of a remaining oxide layer as indicated by the lack of reconstruction spots and the high background intensity.[12,13]

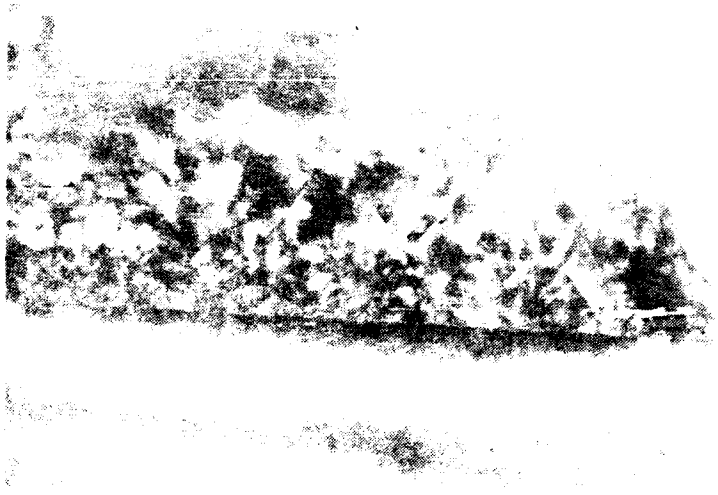

Figure 13. XTEM photograph at the β-SiC/GaN interface. The high density of microtwins/stacking faults diminishes with a few hundred angstroms of growth. Layer is ≈1200Å thick.

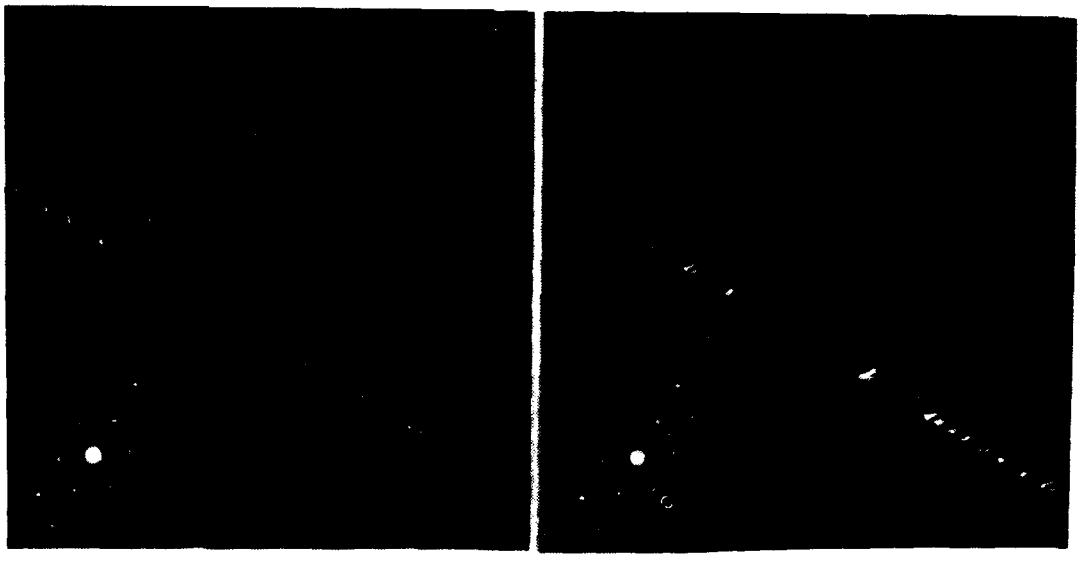

Figure 14. Complementary dark field XTEM images of GaN layer. Inset photographs show the position of the aperture (denoted by the arrow) on the diffraction pattern. The streaks are clearly microtwins/stacking faults on {111} planes.

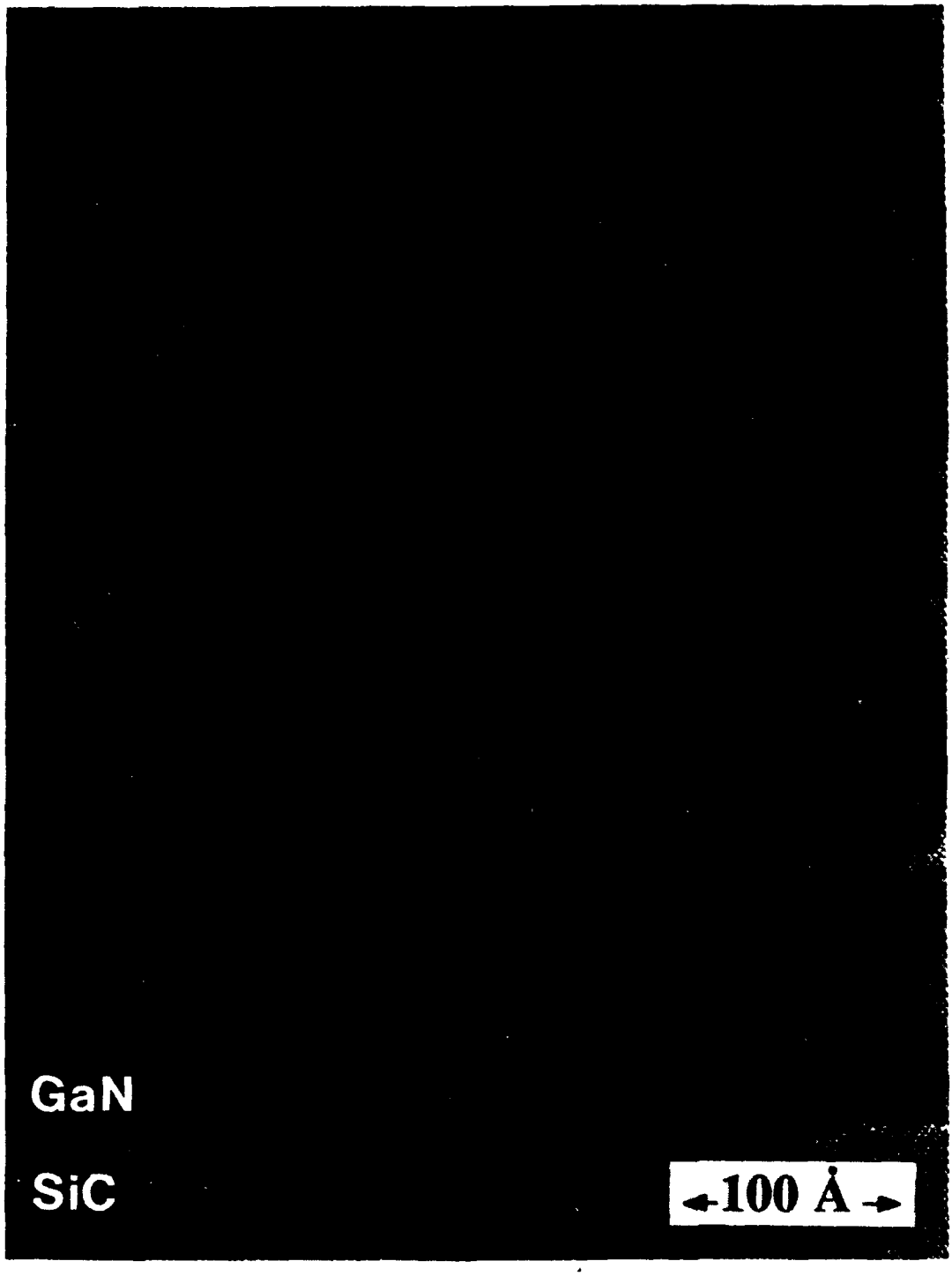

Figure 15. High resolution TEM photograph of GaN film on (100) β-SiC at the interface. Many defects terminate within a few tens of monolayers. Note the thin (3–4 fringes thick) high contrast layer of native oxide at the interface which appears to be the major source of defects.

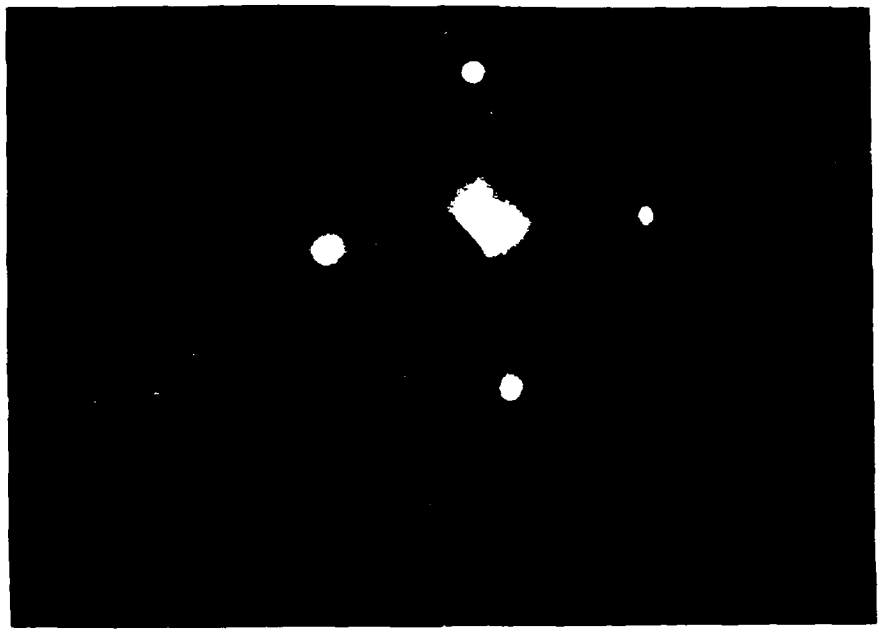

Figure 16. Low energy electron diffraction pattern of (100) β-SiC after vacuum outgassing to 850°C. No evidence of reconstruction and spot splitting with diffuse background indicate presence of remaining thin layer of native oxide on substrate surface.

A comparison of resulting properties of the films grown on the two substrate materials Al_2O_3 (0001) and β-SiC (100) is shown below in Table 2.

Table 2. Typical properties of GaN films grown at 600°C on (0001) Al_2O_3 and (100) β-SiC

Film Property	(0001) Al_2O_3	(100) β-SiC
Est. thickness	30 nm	50 nm
Sheet resistance	450 Ω/	600 Ω/
Resistivity	1.4×10^{-3} Ω-cm	3×10^{-3} Ω-cm
N/Ga ratio	0.78-0.82	0.81-0.86

The N/Ga ratio is somewhat questionable due to variations in results in using elemental sensitivities from different sources (Perkin-Elmer and JEOL). Use of a standard provided by J. Pankove (University of Colorado) did aid in the analysis but more work needs to be done to obtain reliable sensitivity values. This is especially true since preferential sputtering is a possibility, as it has been reported in indium nitride[11] which is a very similar material.

Given the better morphology, higher growth rates, and higher resistivity values it appears that SiC is a better substrate material than sapphire. However, other workers (e.g., reference 15) have reported that the use of a thin buffer layer of AlN has greatly increased the quality of the GaN film grown. Since AlN matches quite well with GaN, the use of a AlN buffer layer might work also well in the case of GaN growth on silicon carbide.

4. Future Research

4.1 Nitrogen Source

Since the films exhibited low growth rates and low resistivity values and often exhibited excess gallium, it seems apparent that the nitrogen source was not producing sufficient amounts of activated nitrogen. It is thought that one problem may be insufficient power transfer from the microwave cavity to the nitrogen gas. This was indicated by the lack of change or even decrease in amount of atomic nitrogen detected by the QMS as the microwave power was increased.

The are a number of alternative approaches that also may be investigated. The use of an electron cyclotron resonance microwave plasma has been used in the growth of GaN.[14] Use of a different source gas is also a possibility. Nitrogen/noble gas mixtures have been used in the deposition of aluminum nitride,[15] and represent an alternative as well. Finally, nitrogen compounds such as ammonia (for example, reference [2]) and hydrazine[16] which are the most common nitrogen sources used. This was originally avoided in an attempt to bypass potential problems with reaction byproducts, but might provide a viable alternative in the relative cleanliness of UHV. In addition, the current ion pump/cryopump system is unsuitable for pumping the large amounts of hydrogen byproducts produced by those sources. Thus the addition of a large turbomolecular pumping package would be required.

4.2 Substrate Materials

Substrate materials continue to be under investigation. Future substrates to be investigated include Si, Ge, and GaAs. Samples of these substrate materials have already been received. These substrates do not have the advantage of close lattice match as does β-SiC, but are much more widely available. In addition, there is a potential for easier removal of native oxide, which would in turn produce a higher quality interface region.

A second effort which will begin shortly is the use of an *ex situ* hydrogen treatment in an effort to reduce the native oxide on the β-SiC substrates.

While an *ex situ* treatment would obviously be less desirable than an *in situ* treatment, the problem of hydrogen pumping mentioned above will initially prevent such tests. Somewhat surprisingly, *ex situ* treatments in a hydrogen atmosphere have proven effective in the growth of other materials such as GaAs.[17]

4.3 Layered Materials

Installation of required equipment and software has been completed to allow the use of ALE. These modifications will also permit the growth of layered materials in the ternary of GaN/AlN/InN. This ternary which has complete solid solubility across the entire range, spans a bandgap range from 1.95 eV for InN to 6.28 eV for AlN. The figure below shows the relationships of bandgap and lattice parameters for the hexagonal form of these materials.

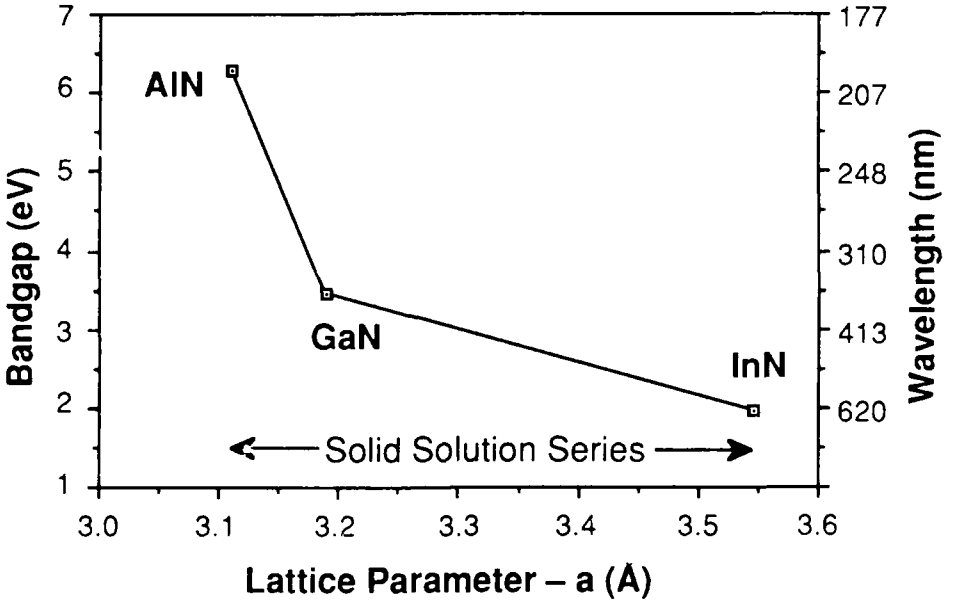

Figure 17. Diagram showing the relationship between lattice parameter and bandgap in the solid solution series of GaN/AlN/InN.

Preliminary growth studies have begun on the individual materials AlN and InN. Once the growth parameters have been determined for deposition of AlN and InN, growth of layered materials can begin.

5. Growth and Analysis Equipment

The RVLEED (Reverse View Low Energy Electron Diffraction) system* has been installed temporarily on the end of the transfer tube of the MBE system to allow its more immediate use in the study of GaN/SiC surfaces. It is also hoped to use the RVLEED in a low resolution AES (Auger Electron Spectroscopy) mode to help characterize the upper surface of substrates and thin films. As shown earlier in the HRTEM photographs, there is a defective boundary layer at the GaN/SiC interface and use of these techniques should help in developing processing methods (such as hydrogen pre-treatment) to remove them.

The analytical chamber has been received from Perkin-Elmer along with many components from their respective suppliers. The support frame for the analytical chamber has also been completed by the machine shop. Initial assembly has begun, and it is expected that the chamber will be under vacuum and undergoing initial tests by the next quarterly report.

Plans for construction of the laboratory facilities in the Centennial campus building are continuing. Equipment to be installed in the labs has nearly all been received. Occupancy is expected early next year.

6. Related Activities

Dr. Davis co-authored a paper entitled "Critical Evaluation of the Status and the Areas for Future Research regarding the Wide Band Gap Semiconductors of Diamond, Gallium Nitride and Silicon Carbide," by R. F. Davis, Z. Sitar, B. E. Williams, H. S. Kong, H. J. Kim, J. W. Palmour, J. A. Edmond, J. Ryu, J. T. Glass, and C. H. Carter, Jr. This paper will be published in the *Journal of Materials Science and Engineering B: Solid State Materials for Advanced Technology*, S. Mahajan and N. Balkanski, eds , Elsevier, New York, 1988. Dr. Davis also made a presentation entitled "Critique Regarding the Status and the Areas for Future Research for the High Temperature Semiconductors of Gallium Nitride and Silicon Carbide," at the Air Force Workshop on High Temperature Electronics, Sandia National Laboratory, April, 12–14, 1988.

Mr. M. J. Paisley presented a paper entitled "Growth of Gallium Nitride Thin Films via Modified MBE Techniques," at the 34th National Symposium of the American Vacuum Society, in Anaheim, California. Mr. Paisley also presented a paper entitled "Growth of Gallium Nitride on Silicon Carbide by Molecular Beam Epitaxy," at the SPIE Optoelectronics

* RVL-8, Princeton Research Instruments, Inc., Princeton, NJ 08542

and Laser Applications in Science and Engineering Conference. This paper was part of the 1988 Innovative Science and Technology Symposium and was published in the proceedings from that meeting.[18]

A paper entitled "Growth of cubic GaN by gas source MBE," by M. J. Paisley, Z. Sitar, J. B. Posthill, and R. F. Davis, has been accepted for presentation at the American Vacuum Society National Symposium, in Atlanta, GA, in October, 1988.

7. References

1. K. Das and D. K. Ferry, Hot Electron Microwave Conductivity of Wide Bandgap Semiconductors, *Solid State Electronics*, Vol. 19, p. 851, 1976.

2. M. Gershenzon, *Evaluation of Gallium Nitride for Active Microwave Devices*, Technical Report, Contract. No. N00014-75C-0295, NTIS No. AD-A099344, 1980.

3. J. A. Thornton in *Deposition Technologies for Films and Coatings*, Chapter 2, R. F. Bunshah, ed., Noyes Publications, Park Ridge, N. J., 1982.

4. Dr. Dennis Manos, Private Communication, Process Plasma Diagnostics Workshop, Princeton Scientific Consultants, May 1987.

5. J. H. Kolts and D. W. Setser in *Reactive Intermediates in the Gas Phase: Generation and Monitoring*, D. W. Setzer, ed., Academic Press, New York, 1979.

6. Bruce McCarroll, "An Improved Microwave Discharge Cavity for 2450 MHz," *Review of Scientific Instruments*, Vol. 41, pp. 279–80, 1970. F. C. Fehsenfeld, K. M. Evenson, and H. P. Broida, "Microwave Discharge Cavities Operating at 2450 MHz," *Review of Scientific Instruments*, Vol. 36, pp. 294–8, 1965.

7. Robert F. Davis, Calvin H. Carter,Jr., M. J. Paisley, and Susan H. Mack, "The Growth of Gallium Nitride via the Innovative Technique of Atomic Layer Epitaxy," Annual Progress Report, ONR Contract #N00014-86-K-0686, June 1, 1987.

8. Robert F. Davis, Calvin H. Carter, Jr., "The Growth of Gallium Nitride via the Innovative Technique of Atomic Layer Epitaxy," Quarterly Progress Report, ONR Contract #N00014-86-K-0686, September 1, 1987.

9. W. Seifert and A. Tempel, "Cubic Phase Gallium Nitride by Chemical Vapor Deposition," *Physica Status Solidi (A)–Applied Research*, Vol. 23, K39–40, (1974).

10. J. I. Pankove , "Luminescence in GaN," *Journal of Luminescence*, Vol. 7, 114–26, (1973).

11. C. P. Foley and J. Lyngdal, "Analysis of indium nitride surface oxidation," *Journal of Vacuum Science and Technology A*, Vol. 5, No. 3, pp. 1708–1712, 1987.

12. Moshe Dayan, "AES and LEED study of the zinc blende SiC(100) surface," *Journal of Vacuum Science and Technology A*, Vol. 3, No. 2, pp. 361–6, 1985.

13. Moshe Dayan, "The β-SiC(100) surface studied by low energy electron diffraction, Auger electron spectroscopy, and electron energy loss spectra," *Journal of Vacuum Science and Technology A*, Vol. 4, No. 1, pp. 38–45, 1985.

14. Sakae Zembutsu and Toru Sasaki, "Low Temperature Growth of GaN Single Crystal Films Using Electron Cyclotron Resonance Plasma Excited Metalorganic Vapor Phase Epitaxy," *Journal of Crystal Growth*, Vol. 77, pp. 250-256, 1986.

15. S. Yoshida, S. Misawa, and S. Gonda, "Improvements on the electrical and luminescent properties of reactive molecular beam epitaxially grown GaN films by using AlN-coated substrates," *Applied Physics Letters*, Vol. 42, No. 5, pp. 427–420, 1983.

16. D. K. Gaskill, N. Bottka, and M.C. Lin, "Growth of GaN films using trimethylgallium and hydrazine," *Applied Physics Letters*, Vol. 48, No. 21, pp. 1449–1451, 1986.

17 T. P Humphreys, K. Das, S. M. Bedair, J. J. Wortman, N Parikh, W. K. Chu, N. El-Masry, and J. C. L. Tarn, Molecular-Beam-Epitaxial Growth of GaAs on High-Temperature Hydrogen-Annealed (100) Silicon, *Electronics Letters*, Vol. 20, No. 23, pp. 1079–81, 1987.

18. M. J. Paisley, Z. Sitar, C. H. Carter, Jr., and R. F. Davis, "Growth of Gallium Nitride on Silicon Carbide by Molecular Beam Epitaxy," In *Micro-Optoelectronic Materials*, Carl A. Kukkonen, ed., pp. 8–12, Proceedings of SPIE, Vol. 877, January 13–14, 1988, Los Angeles, California.

A. Distribution List—Annual Report

Address	No. of Copies
Mr. Max Yoder Office of Naval Research Electronics Program—Code 1114 800 North Quincy Street Arlington, VA 22217	2
Director, Naval Research Laboratory ATTN: Code 2627 Washington, DC 20375	6
Defense Technical Information Center Building #5 Cameron Station Alexandria, VA 22314	14
Dr. J. I. Pankove University of Colorado Department of Electrical and Computer Engineering Boulder, CO 80309	1